Science of the Total Environment 835 (2022) 155455

Contents lists available at ScienceDirect

Science of the Total Environment

journal homepage: www.elsevier.com/locate/scitotenv

Albedo impacts of current agricultural land use: Crop-specific albedo from MODIS data and inclusion in LCA of crop production

Petra Sieber [1,*], Niclas Ericsson, Torun Hammar [2], Per-Anders Hansson

Department of Energy and Technology, Swedish University of Agricultural Sciences (SLU), Uppsala SE750 07, Sweden

HIGHLIGHTS

- Crop-specific albedo under regional conditions was produced from MODIS products.
- Ley and winter crops gave higher albedo than spring crops in wet-temperate climate.
- Climate impacts of albedo change were expressed as radiative forcing.
- Time-dependent LCA was used to assess crop production including albedo and GHGs.
- Albedo increase offset some GHG-induced warming and dominated on short timescales.

GRAPHICAL ABSTRACT

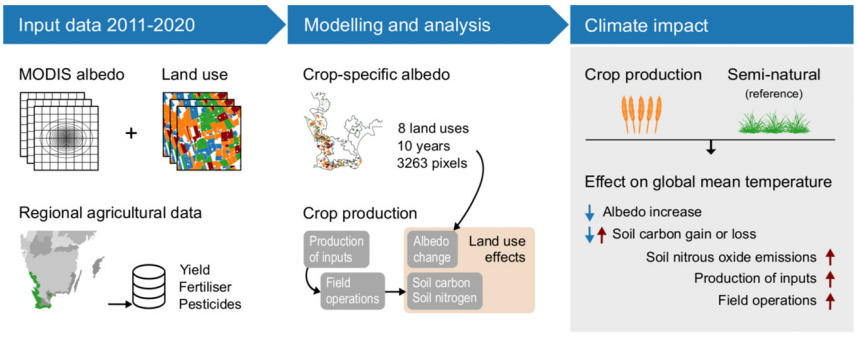

ARTICLE INFO

Editor: Kuishuang Feng

Keywords:
Land cover change
LULUC
Biophysical effects
Climate impact
Albedo
Life cycle assessment

ABSTRACT

Agricultural land use and management practices affect the global climate due to greenhouse gas (GHG) fluxes and changes in land surface properties. Increased albedo has the potential to counteract the radiative forcing and warming effect of emitted GHGs. Thus considering albedo could be important to evaluate and improve agricultural systems in light of climate change, but the albedo of individual practices is usually not known. This study quantified the albedo of individual crops under regional conditions, and evaluated the importance of albedo change for the climate impact of current crop production using life cycle assessment (LCA). Seven major crops in southern Sweden were assessed relative to a land reference without cultivation, represented by semi-natural grassland. Crop-specific albedo data were obtained from a MODIS product (MCD43A1 v6), by combining its spatial response pattern with geodata on agricultural land use 2011–2020. Fluxes of GHGs were estimated using regional data and models, including production of inputs, field operations, and soil nitrogen and carbon balances. Ten-year mean albedo was 6–11% higher under the different crops than under the reference. Crop-specific albedo varied between years due to weather fluctuations, but differences between crops were largely consistent. Increased albedo countered the GHG impact from production of inputs and field operations by 17–47% measured in GWP_{100}, and the total climate impact was warming. Using a time-dependent metric, all crops had a net cooling impact on global mean surface temperature on shorter timescales due to albedo (3–12 years under different crops), but a net warming impact on longer timescales due to GHG emissions. The methods and data presented in this study could support increasingly comprehensive assessments of agricultural systems. Further research is needed to integrate climatic effects of land use on different spatial and temporal scales, and direct and indirect consequences from a systems perspective.

* Corresponding author at: Department of Energy and Technology, Swedish University of Agricultural Sciences (SLU), PO Box 7032, Uppsala SE750 07, Sweden.
E-mail addresses: petra.sieber@env.ethz.ch (P. Sieber), niclas.ericsson@slu.se (N. Ericsson), torun.hammar@ri.se (T. Hammar), per-anders.hansson@slu.se (P.-A. Hansson).
[1] Present address: Institute for Atmospheric and Climate Science, ETH Zurich, Zurich, Switzerland.
[2] Present address: RISE Research Institutes of Sweden, Stockholm, Sweden.

http://dx.doi.org/10.1016/j.scitotenv.2022.155455
Received 14 April 2021; Received in revised form 6 April 2022; Accepted 19 April 2022
Available online 23 April 2022

1. Introduction

The recent IPCC Special Report on Climate Change and Land (IPCC, 2019b) highlighted the effect of land use on climate due to changes in surface characteristics. Considering biophysical climate effects could be important to evaluate and improve land use practices, biomass-based systems, and response options intended to mitigate and adapt to global warming (Bagley et al., 2015; Georgescu et al., 2011; Marland et al., 2003). The present study focuses on effects of agricultural land use on surface albedo, the fraction of solar radiation reflected back from the ground. Albedo change alters surface energy and moisture budgets, and can thereby influence temperatures and the hydrological cycle at local to regional scale (Mahmood et al., 2014; Pielke et al., 1998). Furthermore, albedo change directly perturbs Earth's radiative balance at the top of the atmosphere (TOA) and thus exerts a radiative forcing (RF) on the global climate system.

Calculated RF provides a simple means to quantify and compare the contribution of diverse forcing agents to global mean temperature change (Myhre et al., 2013). RF can be useful to evaluate the importance of albedo change in relation to greenhouse gas (GHG) emissions and carbon sequestration (Betts et al., 2007), while minding the specific limitations of the RF concept when assessing land use climate impacts (Bright and Lund, 2021; Davin and de Noblet-Ducoudré, 2010; Marland et al., 2003; Pielke et al., 2002). RF of albedo change is increasingly included in assessments of land use climate impacts, either exclusively (Betts, 2000; Chang et al., 2021; Smith et al., 2016) or jointly with local biophysical effects (e.g. Georgescu et al., 2011; Zhao and Jackson, 2014). The growing interest to evaluate and improve agricultural systems in light of climate change has added to this development. To support decisions, an understanding of potential land use effects is needed, including changes to land surface characteristics such as albedo. However, albedo is often approximated by generic values that fail to represent individual crops and management practices and to differentiate environmental conditions.

The albedo of land depends on soil properties (e.g. texture, organic matter content, moisture), vegetation properties (e.g. leaf and stem reflectance, orientation, density) and deposition of water, snow or particles (Bright et al., 2015). These factors are influenced by climate and weather (e.g. temperature, precipitation), plant phenology (e.g. emergence, maturity, senescence) and human interventions. Agricultural land use affects albedo by crop types and varieties grown (Miller et al., 2016; Singarayer and Davies-Barnard, 2012; Starr et al., 2020), and management practices such as residue retention, tillage and cultivation of cover crops (Davin et al., 2014; Kaye and Quemada, 2017). These agricultural practices can lead to differing albedo under the given environmental conditions. However, data gaps and uncertainty remain about how individual agricultural practices affect albedo, depending on soil properties and local climate (Bagley et al., 2015; Erb et al., 2017). Such knowledge could be useful, especially to inform management recommendations or policies that incentivise specific practices.

Albedo is well-characterised at the level of land cover classes, such as cropland and grassland. Distinguishing between crops and management practices is challenging due to the dependence of albedo on environmental factors, and lack of robust data to account for this dependence. Field stations provide high-resolution measurements of albedo in specific fields with known land use, often spanning multiple years. However, their coverage is insufficient to capture and disentangle the combined effects of temperature, precipitation, soil type, crop and management in any chosen region. Remote sensing offers consistent long-term records of surface reflectance at global scale, which are used continuously to estimate albedo at regular intervals and to produce gridded data products (Qu et al., 2015). Moderate Resolution Imaging Spectroradiometer (MODIS) albedo products provide daily albedo values and model parameters that capture rapid surface dynamics induced by seasonal vegetation development, human interventions and snow cover (Wang et al., 2018). Data are available from 2000 to present with nine days lag. MODIS products were used to characterise the albedo of contrasting land cover classes globally (Gao et al., 2005) and regionally (Wickham et al., 2015), and to model the impact of land cover change on RF (Myhre et al., 2005) or local temperature (Duveiller et al., 2018). However, implementing surface classifications at the level of individual crops is challenging. First, accurate maps of yearly crop cultivation are not easily available (see e.g. methods in Starr et al., 2020). Second, linking MODIS albedo directly to surface conditions requires the signal of individual pixels to be composed of observations over a homogeneous area, which becomes increasingly difficult for smaller land units (see e.g. Hovi et al., 2019). Crop fields in heterogeneous agricultural landscapes in Europe often have a size of a few hectares, whereas grid cells of MODIS albedo products are representative of an area of 833 m × 618 m at European mid-latitudes (Campagnolo et al., 2016).

The objectives of this study were to (1) quantify the albedo of individual crops under regional production conditions (i.e. soil type, climate, management practices), using the MODIS product MCD43A1 v6, and (2) assess the importance of albedo change for the climate impact of current crop production in terms of RF, using life cycle assessment (LCA).

2. Materials and methods

2.1. Scope of the study

An agricultural region in southern Sweden was chosen as a study area. Ten years of MODIS data were used to produce representative climatological daily and annual albedo per crop. Seasonal patterns in albedo, and variability across crops, years and sites, were analysed. Crop-specific albedo has a range of scientific applications, notably to assess effects of land use on different climate variables at local or global scale. Here, RF was calculated to assess the importance of albedo change for the climate impact of crop production. Life cycle assessment was performed considering GHG fluxes along the supply chain and due to land use, relative to a land reference without cultivation. This is one possible approach to assess albedo-related effects of agricultural land use. Inclusion of albedo in LCA could have various applications, since LCA is widely used to evaluate biomass-based product systems (e.g. food, biofuels and biomaterials) with increasing consideration of land use effects.

2.2. Study area and agricultural land use

The study included seven major crops (winter wheat, winter rye, winter rape, spring wheat, spring barley, sugar beet and ley) cultivated in Sweden's southernmost agricultural production region (PO1) (Fig. 1). These crops

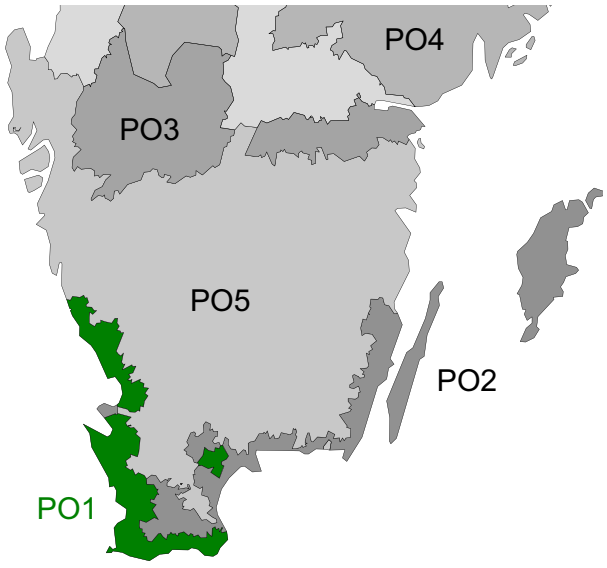

Fig. 1. Location of the study area, agricultural production region PO1 (green) in the south of Sweden.

together account for 80% of agricultural land use in the PO1 region (Statistics Sweden, 2020b). PO1 is one of eight production regions in Sweden, each of which is characterised by specific production conditions in terms of topography, climate and soil type. PO1 has a wet-temperate climate, with mean annual temperature of 7.8 °C, mean annual precipitation of 757 mm and sandy loam and loam as prevalent soil types (Andrén et al., 2008). The vast majority of crop production is rainfed. Despite its small area, PO1 accounts for a large proportion of Sweden's total crop harvest, supplying almost 30% of winter wheat and spring barley, over 40% of rapeseed and over 80% of sugar beet (Statistics Sweden, 2020a). Unimproved grassland, i.e. permanent grassland on agricultural land that is not fertilised and grazed extensively (Velthof et al., 2014), was included as a proxy for the land reference without crop cultivation. In southern Sweden, unimproved (often semi-natural) grassland is dominated by herbaceous vegetation suitable for grazing, with scattered occurrence of shrubs and deciduous trees.

2.3. Albedo and radiation data

Surface albedo was derived from the MODIS product MCD43A1 v6, provided daily on a regular grid with 463 m pixel size. Representative pixels for each land use were identified using the Python package GeoPandas (Jordahl et al., 2020). The footprint of each albedo pixel, i.e. the surface area generating its signal, was compared with agricultural land use reported in 2011–2020 (harvest years). Pixels with a signal originating to at least 85% from agricultural land and 80% from a single crop were selected. These thresholds were set empirically to achieve high pixel purity while maintaining a representative sample of different pixels for each crop and year.

For the selected pixels of each crop and harvest year, daily albedo model parameters were retrieved for the growing season and possibly a period outside the growing season, to cover a full year (Fig. 2). The period outside the growing season is not crop-specific and therefore daily albedo before sowing was averaged across spring crops, and after harvesting across cereal crops. The climatological (10-year) mean albedo per crop was obtained by averaging first across pixels and then across years. This ensured equal weighting of years with potentially different growing conditions.

2.3.1. Land use data

Polygon layers of agricultural production regions and fields were obtained from the Swedish Board of Agriculture. The field layer is an output of applications for subsidies under the European Union (EU) Common Agricultural Policy (Swedish Board of Agriculture, 2020). Farmers in each EU member state declare their agricultural parcels in a national online portal, by providing both geospatial and land use information. The resulting Geospatial Aid Application (GSAA) data include single crops or crop groups with equal payment eligibility, and are validated by authorities through comparison against reference parcels in the Land Parcel Identification System (LPIS), field visits and remote sensing (Sagris et al., 2013). The definition and distinguished types of permanent grassland vary among member states, depending on environmental conditions and established practice. Sweden prohibits fertiliser application on permanent grassland and allows up to 50% fractional cover of shrubs, trees or impediments. Most permanent grassland was never ploughed and can be considered semi-natural.

2.3.2. Pixel footprint model

MODIS Bidirectional Reflectance Distribution Function and Albedo (BRDF/Albedo) products are produced using high-quality reflectance observations from Terra and Aqua satellites during a 16-day moving window. BRDF estimates assigned per day and pixel are based on observations from multiple days and angles, resulting in a footprint that is larger than suggested by the product's 500 m nominal resolution (Campagnolo et al., 2016). The footprint is the combined result of the MODIS imaging system (sensor properties and scan geometry) and the spatial and temporal sampling procedures applied to generate a gridded daily product (Campagnolo and Montaño, 2014). Consequently, each BRDF/Albedo value has a specific footprint and the exact footprint is usually not known.

The footprint can be restricted by utilising knowledge of the spatial response characteristics of the MODIS product. Similar to Hovi et al. (2019), we applied an elliptical Gaussian point spread function to describe the surface area that contributes to each pixel in terms of size, shape and response distribution. Function parameters were based on a median effective resolution of 833 m × 618 m estimated at a site in the Netherlands (Campagnolo et al., 2016), which gives a good indication of the situation in southern Sweden (see Fig. 12, Campagnolo and Montaño, 2014). The effective resolution was measured by the length on the ground that on average produces 75% of the signal along the x and y dimensions (D75%), and can be related to the shape of a Gaussian function using $\sigma = 1.0235 \times D75\% / 2.355$.

Gaussian functions for the x and y dimensions were sampled at 20 levels, from which the dimensions of elliptical rings around the pixel centre with 5% coverage each were obtained. The further a ring is from the pixel centre, the larger its area and the lower the contribution of one square metre to the signal. The relative contribution was expressed in an area-based weighting factor for each ring, $w = 0.05 \times$ Total area / Ring area. Total area was truncated at 99.5%, corresponding to 240 ha or ellipse dimensions of 2033 m × 1508 m in the x and y direction, respectively. For each pixel and land use, the rings were intersected with relevant field polygons and pixel purity was calculated as the weighted sum of intersecting areas. Pixels were considered sufficiently pure if at least 80% of the signal originated from the land use of interest. To reach 80% purity, a crop had to cover at least 50 ha in proximity to the pixel centroid (Fig. 3).

2.3.3. Albedo data

Daily mean blue-sky albedo was calculated using the MODIS BRDF/Albedo model parameters product MCD43A1 v6 (Schaaf and Wang, 2015).

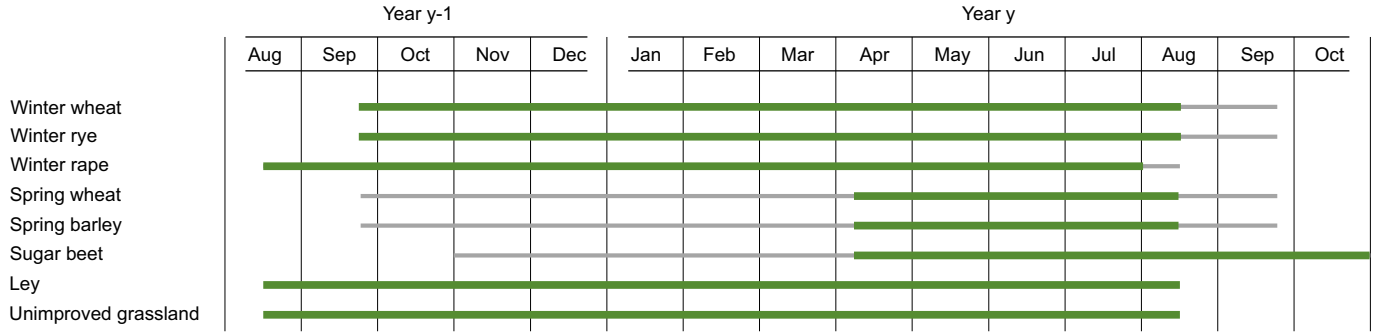

Fig. 2. Growing season under normal weather conditions in Swedish production region PO1 (green bars). For annual crops, the growing season started with sowing and ended with harvesting in year y. For winter crops, the season starts in autumn of the previous year (y-1). Grey bars mark periods outside the growing season that were included and assigned to harvest year y.

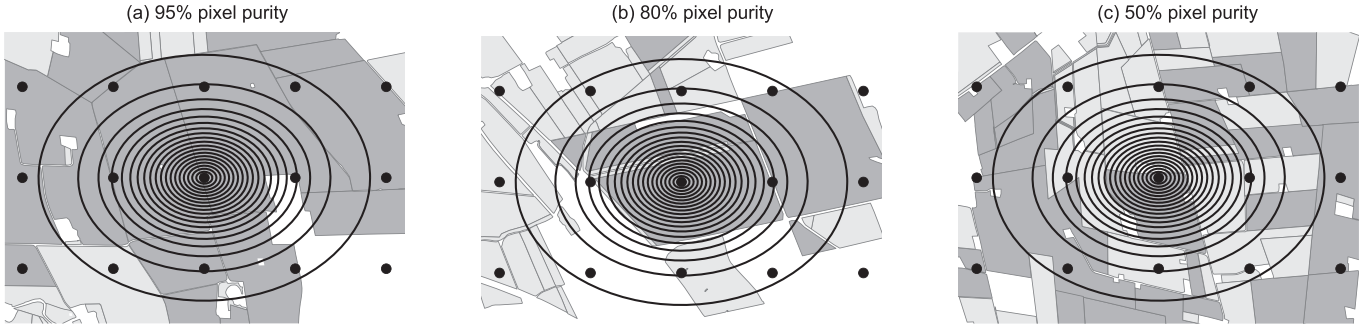

Fig. 3. Candidate pixels for winter wheat with different purity and distribution of fields (yellow) in the footprint area: (a) 95% purity, mainly winter wheat; (b) 80% purity, winter wheat in proximity to the pixel centroid; and (c) 50% purity, winter wheat mixed with other agricultural land (grey). Black dots indicate pixel centroids of the MODIS BRDF/Albedo product with 463 m distance in the x and y direction. Elliptic rings around the candidate pixel's centroid each represent 5% of the pixel's footprint.

Blue-sky albedo refers to albedo under actual illumination conditions with a combination of diffuse and direct radiation at a given time. White-sky albedo (WSA) and black-sky albedo (BSA) represent albedo under completely diffuse and direct illumination, respectively, and are not recommended as a surrogate for daily mean albedo (Wang et al., 2015). The BRDF model parameters allow surface albedo to be estimated at any illumination geometry during daytime.

The BRDF parameters for the shortwave broadband (0.3–5.0 μm) and coefficients for the isotropic, volumetric and geometric kernel integrals were used to compute hourly BSA as a function of solar zenith angle (SZA) and daily WSA (Schaaf et al., 2002). Blue-sky albedo was calculated as a linear combination of WSA and BSA weighted by the instantaneous fraction of diffuse and direct surface irradiance (Lewis and Barnsley, 1994). As this relationship breaks down at high SZA (Liu et al., 2009; Lucht et al., 2000), it was used for SZA over 70° only on winter days (31 October to 11 February), when the sun does not rise higher than 20° in southern Sweden. Daily mean blue-sky albedo was calculated as the average of hourly values weighted by total surface irradiance (Wang et al., 2015).

The BRDF parameters from full inversions (based on sufficient high-quality MODIS observations) and magnitude inversions (based on a back-up algorithm) were used in our calculations. Magnitude inversions of poorer quality often provide reliable results, and their accuracy has been further improved in version 6 of MCD43 by using the latest full inversion as pixel-specific a priori knowledge (Wang et al., 2018). When there were too few clear sky observations for retrieving the BRDF, which occurred mainly in winter, the gaps were filled by linear interpolation for each site and year before aggregation across pixels.

2.3.4. Atmospheric data and radiative transfer

Shortwave radiation fluxes and atmospheric properties were derived from the ERA5 global reanalysis dataset (Hersbach et al., 2018). Variables were retrieved at the native grid resolution of 31 km and averaged regionally using a gridded mask over PO1. Hourly data were averaged across the same 10 years as used for albedo retrieval (mid-2010 to mid-2020) to generate standard atmospheric conditions. Data on hourly direct and total surface irradiance were employed in calculation of daily mean blue-sky albedo.

The impact of surface albedo on the TOA radiation balance was estimated using an isotropic single-layer model of the atmosphere. This technique is commonly used to study surface-atmosphere interactions based on known boundary fluxes from climate models or observations (Donohoe and Battisti, 2011; Stephens et al., 2015; Winton, 2005). The simplifying assumption that the same fraction of radiation is reflected or absorbed on each pass through the atmosphere generally tends to underestimate transmittance, but has proven reasonable in the mid-latitudes (Donohoe et al., 2020). Here, net and downwelling radiation at the surface and at the TOA from ERA5 were used to calculate daily atmospheric transmittance and reflectivity. These atmospheric properties were needed to model radiative transfer of incoming and reflected radiation through the atmosphere, and to compute annual mean RF from albedo change (Sieber et al., 2020).

2.3.5. Data analysis

Land cover type and properties of the pure pixels were crosschecked against the MODIS Land Cover Type Product MCD12Q1 version 6 (Friedl and Sulla-Menashe, 2019), which is provided yearly on the same grid as albedo. Checks were made on how pure pixels for each crop were classified according to different schemes. Pixels with cereals and sugar beet were almost exclusively classified as herbaceous annuals cultivated with cereal or broadleaf crops. Leys were classified as cereal cropland, grassland or a combination of both. Pixels with unimproved grassland were assigned different types indicating a mix of grass, shrub and tree cover. This agrees with the Swedish GSAA categories used for permanent grassland.

Two-way ANOVA was used to investigate whether land use and yearly weather conditions affected annual albedo across pure pixels, and whether there was a significant interaction effect ($p < 0.05$). Post hoc paired comparisons were conducted with Tukey's test. A linear mixed effects model was fitted to investigate the effect of land use on annual albedo, while controlling for the variation between years. This approach utilised all data, irrespective of missing observations for a land use in a year. Land use was handled as a fixed effect factor with eight levels (i.e. seven crops and unimproved grassland), and year as random effect factor with sampled levels (i.e. weather conditions 2011–2020). The regression assumptions of normality and homoscedasticity were validated using normal probability and residual plots.

2.4. Life cycle assessment

LCA was performed to get a perspective on the importance of albedo relative to the GHG-related climate impact of crop production on current cropland, per hectare land. The seven crop production scenarios each represented a single cultivation year under average production conditions in PO1 (soil, climate, yield level) and common farming practice (inputs, field operations). Nutrient supply by mineral fertilisers was assumed. For simplicity, application of manure, urea or limestone, and irrigation were excluded. The system boundaries included production of inputs, fuel consumption for field operations and land use effects due to changes in albedo, soil carbon (C) and soil nitrogen (N) balance during the cultivation year (Fig. 4). Crop residue management was considered, but not post-harvest handling of the crop. Production and maintenance of machinery were not accounted for.

Land use effects of crop production were studied relative to a situation without cultivation. Permanent grassland with occurrence of shrubs and trees is a realistic medium-term situation of non-use in southern Sweden,

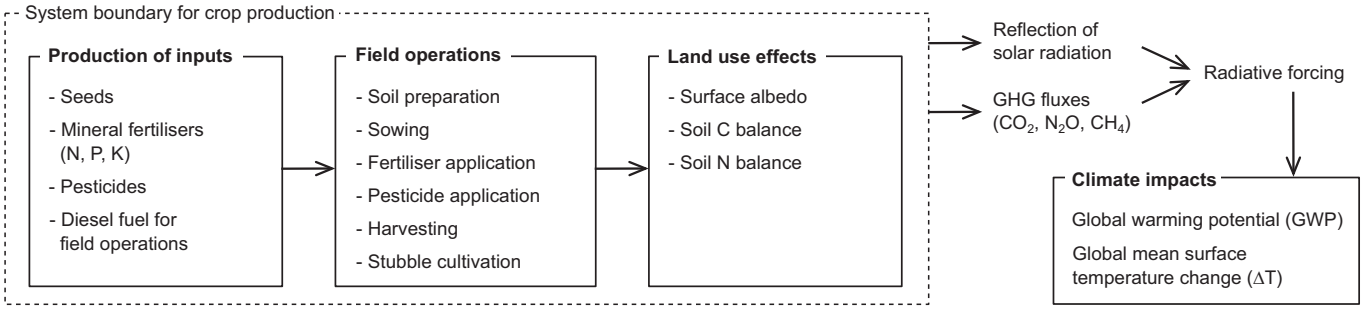

Fig. 4. System boundary and processes included in life cycle assessment of crop production. Impacts on climate due to albedo and greenhouse gas (GHG) emissions were measured with two climate metrics.

resembling semi-natural grassland. The land reference was modelled using albedo of unimproved grassland produced in this study, and assuming emission of 0.3 kg N_2O-N ha^{-1} yr^{-1} (Kim et al., 2013) and stable soil carbon stocks. In the results section, land use effects are presented relative to the reference and in absolute terms (i.e. as the difference to a hypothetical reference with albedo of 0 and no emissions), to show the influence of the chosen reference situation on the results. All crops were assumed to require land for a whole year because only one main crop can be sown and harvested per year in Sweden. Inputs, field operations and land use effects were considered on a yearly basis in the life cycle inventory analysis. Land use effects during the cultivation year were assessed due to RF from albedo change relative to the reference, and soil N_2O emissions and soil C accumulation or loss under individual crops on current cropland, relative to baseline emissions of the reference. This means that only flows during the time of cultivation were accounted for, similar to the methods in Brandão et al. (2011). The crop production scenarios were not attributed any burden for historical land conversion or delayed future regeneration.

2.4.1. Field operations and inputs

Field operations and inputs required for cultivation of each crop in PO1 were based on 10-year average yields (Statistics Sweden, 2020a), common farming practices and recommendations for the given growing conditions, expected yield and quality (Kvarmo et al., 2019). Wheat, rye, rape and sugar beet are primarily grown as food crops in Sweden, whereas barley is mainly grown for fodder. Ley includes grass-clover mixtures grown temporarily on arable land in a crop rotation. Three harvests of ley per year and termination after two years were assumed, corresponding to medium to intensive management without grazing. Because statistical yield data for ley include partially grazed and extensive leys, a higher suitable yield of 8 Mg DM ha^{-1} was used. A fraction of the crop residues was exported, 45% of straw for cereals and 10% of residues for rapeseed. Inventory data and references for activities, inputs and emissions are provided in Tables S1-S4 in the Supplementary Material.

Field operations assumed included ploughing, harrowing, conventional or combined sowing, fertiliser application, pesticide application, harvest and stubble cultivation. Type of field operations and number of machine passes were differentiated by crop. Diesel consumption was determined for each operation. Diesel consumption for ploughing was calculated as a function of soil clay content, and for threshing of cereals and rape as a function of yield (Table S2).

Nitrogen was assumed to be supplied by mineral fertiliser according to recommended amounts for each crop (Table S1). The amount of applied fertiliser was decreased for rapeseed, sugar beet and ley by the reduction in fertiliser requirement they gave rise to in the following season (Kvarmo et al., 2019). Inputs of phosphorus (P), potassium (K) and pesticides were obtained from statistics disaggregated by crop and region. European emissions data on production of mineral fertilisers and pesticides were used (Table S4). Emissions from production of seeds were calculated as a fraction of total emissions, based on yield and seed rate.

2.4.2. Land use effects

Annual RF from albedo change was calculated from climatological (10-year mean) daily values for albedo ($\Delta\alpha = \alpha_{crop} - \alpha_{ref}$) and atmospheric properties (Section 2.3.4).

Nitrous oxide (N_2O) emissions resulting from addition of N to soil were calculated following the IPCC Guidelines for National Greenhouse Gas Inventories (IPCC, 2019). Additions of N through mineral fertiliser and above- and belowground crop residues were considered. Country-specific factors from Sweden's National Inventory Report (Swedish EPA, 2019) were used to estimate N additions from crop residues, and fraction of N leached or volatilised. Direct N_2O emissions and indirect N_2O emissions following leaching and volatilisation were calculated using disaggregated emission factors for a wet-temperate climate from IPCC (2019). Uncertainties in emission factors were considered based on the 95% confidence interval (Table S3a-b).

Accumulation or loss of carbon in the top 25 cm of the soil (i.e. the ploughed layer) were estimated using the ICBM regional model (Andrén et al., 2004) with updated parameter values (Table S3c). Measured topsoil carbon mass averaged across arable soils in PO1 (Andrén et al., 2008) was used as the starting condition. The initial stock of 70.8 Mg C ha^{-1} was split into a young (labile) and an old (stable) pool, as described by Kätterer et al. (2008). Carbon inputs from above- and belowground crop residues were calculated in relation to carbon in the yield (Table S3d). For each crop, the soil C balance was simulated for 100 years with constant inputs, representing sustained cultivation under current conditions. Because the rate of change is high in the first few years and declines over time, the annual average accumulation or loss per cultivation year was calculated and used when assessing a single cultivation year. This approach attributes the long-term development of the soil C balance to individual crops by considering crop-specific C inputs and cultivation intensity, and disregards the timing of crop cultivation and C gains and losses within the 100-year timeframe. Sensitivity to the chosen timeframe was tested by calculating the annual average change over 100 years (default), 50 or 20 years (Table S3d). Model uncertainty could not be quantified because the ICBMr parameters used belong to an internally consistent deterministic calibration.

2.4.3. Climate impact assessment

Climate impacts were assessed using time-dependent LCA methodology originally developed for GHG (Ericsson et al., 2013) and expanded for albedo (Sieber et al., 2020). The method accounts for the RF profiles of GHG fluxes and albedo changes over time, allowing better comparison of climate impacts across forcing agents. Climate impacts were expressed as global mean surface temperature change (ΔT) over 100 years, and as GWP using a 100-year time horizon. GWP characterisation factors used were 1, 36 and 298 kg CO_2e per kg CO_2, fossil CH_4 and N_2O, respectively (Myhre et al., 2013), and 10.9×10^{12} kg CO_2e per unit (1 Wm^{-2}) and year RF from albedo change (Sieber et al., 2020).

3. Results

3.1. Albedo

Geospatial analysis identified 3326 pure pixels in PO1 across 10 years. Pixels in proximity to the sea (<650 m away) showed a negative bias in albedo and were discarded. The final sample contained 3263 pixels, with the highest numbers for winter wheat, spring barley, winter rape and sugar beet (Fig. 5). These crops are common in PO1 and are often grown in rotation on the same fields, which resulted in different sample sizes per crop and year (Tables S6). Numbers were lower but more stable across years for perennial ley and unimproved grassland. No pure pixels were found for winter rye in 2018 and spring wheat in 2011 and 2020.

Daily albedo showed distinct seasonal patterns by type of agricultural land use (Fig. 6). Annual crops led to low albedo (0.12–0.14) outside the growing season, when the bare soil was exposed. Plant cover had higher reflectance than the loam soil, and albedo increased as the crops developed (from 0.15–0.16 in April to 0.20 in June). Rapeseed is a broadleaf crop and provided better soil coverage than cereals or grasses in spring and autumn, leading to higher daily albedo. Ley showed high albedo throughout the year, due to its permanent and dense vegetation. Unimproved grassland had stable albedo throughout the year, but at a low level, possibly due to less dense herbaceous vegetation than on fertilised cropland and the occurrence of shrubs or trees. Temperature and precipitation affected soil moisture and plant growth (cf. Sütterlin et al., 2016). Effects on albedo were stronger for bare or sparsely vegetated land. Rain led to an abrupt temporary decrease, while snowfall led to an increase in albedo.

Among the agricultural land uses studied, climatological (10-year mean) annual albedo was lowest for unimproved grassland (0.172) (Table 1). Ley had the highest albedo (0.190), followed by winter rape (0.188) and winter wheat (0.186). Differences between crops were smaller than 0.01 in the climatological mean, with a tendency for higher albedo of ley and winter varieties than spring varieties. These differences were higher in in individual years, with 0.009–0.018 difference between the crop with the highest and the lowest albedo per year.

Inter-annual variability in albedo was high, with 0.015–0.022 difference between the years with the highest and the lowest albedo per land use. However, inter-annual differences were largely consistent across land uses (Fig. 7, 2011–2020). Compared with the climatological means, albedo levels were elevated in harvest years 2013 and 2018. Both years had many days with snow cover and the snow cover lasted until April, which had a particularly high impact on annual albedo due to increasing incoming radiation in spring. Harvest years 2014 and 2020 had few days with snow cover, and hence low annual albedo levels. Effects of rainfall and temperature differed between crops and were mainly important on seasonal timescales. For instance, the severe growing season drought in 2018 led to increased summer albedo (July until harvest in early August) on winter wheat (+23%, SD = 14%), spring barley (+15%, SD = 13%) and rapeseed (+20%, SD = 13%), decreased summer albedo on ley (−5%, SD = 4%), and no clear effect on sugar beet (+5%, SD = 10%) and unimproved grassland (−6%, SD = 10%). This contrasting effect can be related to differences in vegetation status and response to water stress, soil drying and the fraction of exposed soil. Water stress in plants typically leads to higher reflectance in the visible spectrum due to reduced absorption by chlorophyll, and lower reflectance in the near-infrared spectrum due to changes in leaf cell structure (Sütterlin et al., 2016). Enhanced soil drying increases reflectance, but greater soil exposure due to changes in leaf orientation can decrease albedo if the dry soil is darker than the vegetation. Thus drought gives rise to several opposing mechanisms which can vary in strength and cause differing albedo anomalies for various land cover types and regions (Sütterlin et al., 2016). The differences in summer albedo identified here may not be representative for drought conditions in general.

Variability in annual albedo due to agricultural land uses and yearly weather conditions was analysed using statistical methods (Table S7). ANOVA and Tukey test were restricted to the six land uses with samples from all years. Land use, yearly weather conditions and their interaction had a significant effect on pixel level albedo. Pairwise comparisons of land uses across years were significant for all pairs except ley-winter rape and spring barley-sugar beet. No pair had significantly different means in all years, but most pairs had for 6–9 out of the 10 years. When controlling for inter-annual differences in the linear mixed effects model, all land uses were significant predictors of pixel level albedo. Inter-annual differences explained 30% of the remaining variance. Unexplained differences between pixels of the same land use and year were attributable to management (e.g. fertilisation, field operations, residue management, grazing), site conditions (e.g. soil properties, slope) and pixel composition (e.g. albedo of impurities, shading by surrounding elements).

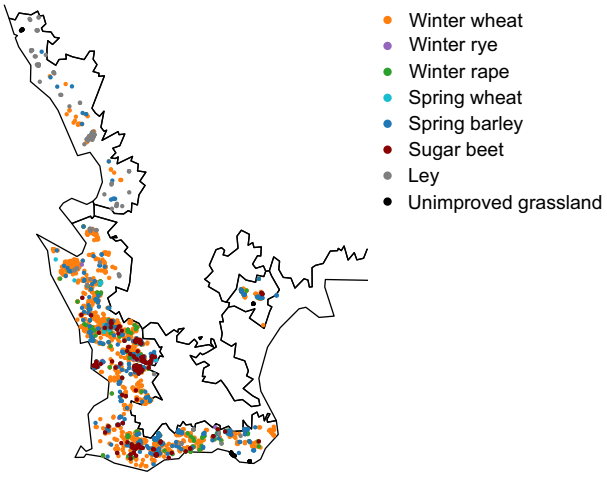

Fig. 5. Location of the crop-specific MODIS albedo pixels in Swedish production region PO1 included in the analysis.

3.2. Life cycle climate impact

All crop production scenarios had a warming impact on climate relative to the land reference. Net climate impacts quantified with GWP_{100} ranged from 0.51 t CO_2e ha^{-1} for ley to 2.46 t CO_2e ha^{-1} for spring wheat (Table 2). Under different crops, albedo increase by 6–11% relative to the reference countered the GHG impact from production of inputs and field operations by 17–47%.

The absolute climate impact due to land use was lowest for the reference despite low albedo (Fig. 8). Soil N was the only GHG source and N_2O emissions were minimal. Among the crop production scenarios, the potential for albedo-related cooling was highest for ley and winter crops. In all scenarios, the single largest contributor to emissions was soil N due to formation of N_2O from applied fertiliser and crop residues. The impact from soil N was largest for crops with high mineral N demand (e.g. winter wheat, with −20% to +23% combined model uncertainty) or high inputs of N-rich residues (e.g. sugar beet, with −56% to +95% uncertainty). Direct N_2O emissions from N in crop residues contributed most to this uncertainty. Soil acted as a CO_2 sink under ley and rapeseed due to high productivity and C inputs, particularly from roots. Under all other crops, the long-term soil C balance was negative, i.e. mineralisation outweighed C inputs over a 100-year timeframe. Using a long timeframe implied that the slow but lasting dynamics in the stable C pool gained importance relative to the fast but temporary dynamics in the labile pool. This partly addressed the issue that labile C is lost quickly when agricultural practices change, e.g. when practices with high C inputs are followed by practices with lower C inputs. Shortening the timeframe to 50 years increased the annual average soil carbon stock change by 10–33% for individual crops. Over a 20-year timeframe, the annual average change could be higher or lower for different crops. These different sensitivities among crops resulted from varying amounts and qualities of C inputs (i.e. aboveground residue and root C).

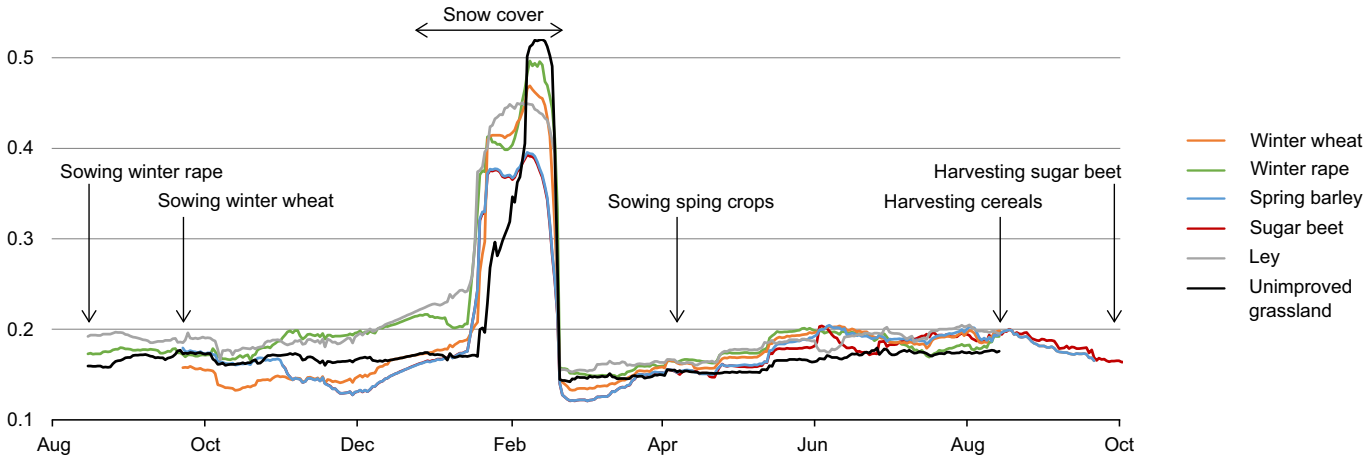

Fig. 6. Daily albedo in the harvest year 2012 (August 2011 to October 2012) under different agricultural land uses.

Table 1
Climatological annual albedo per land use in Swedish production region PO1, calculated from 10 years of MODIS data. Inter-annual variability is given by standard deviation (SD) and coefficient of variation (CV) calculated from annual means per land use. Inter-pixel variability is given by SD calculated from pixel level albedo with annual means subtracted, and CV calculated per year and averaged.

	Albedo	Inter-annual SD	Inter-annual CV	Inter-pixel SD (normalised)	Inter-pixel CV (averaged)
Winter wheat	0.186	0.0065	0.035	0.0084	0.045
Winter rye	0.181	0.0053	0.029	0.0051	0.023
Winter rape	0.188	0.0050	0.027	0.0093	0.049
Spring wheat	0.182	0.0063	0.034	0.0038	0.017
Spring barley	0.183	0.0051	0.028	0.0057	0.029
Sugar beet	0.181	0.0054	0.030	0.0071	0.036
Ley	0.190	0.0069	0.036	0.0080	0.042
Unimproved grassland	0.172	0.0061	0.035	0.0088	0.045

When expressed as the time-dependent metric ΔT, all single-year crop production scenarios had a net cooling impact on global mean surface temperature on short timescales (from 3 years for spring wheat up to 12 years for ley) and a net warming impact on longer timescales. The short-term cooling response resulted from albedo change, which led to high climate forcing during the cultivation year. After the cultivation year, there was no lasting forcing from albedo change and the cooling effect diminished quickly (Fig. 9a for ley). Temperature impacts from production of inputs, field operations, soil C and soil N balance were initially weaker, but increased over time and remained high for decades after cultivation. This resulted from the long atmospheric lifetime of GHGs, especially CO_2, which led to long-lasting RF although there were no new emissions or removals.

Assessing a single cultivation year is useful from a product perspective, because results per hectare and year can be used to relate the calculated impacts to yields. From a land use perspective, effects of sustained production are also relevant. Crop cultivation during 30 years was modelled by assuming the same albedo change and GHG sources every year of the study period, while considering annually varying soil carbon changes as obtained from ICBM. Sustained albedo change led to constant RF over time and thus a stabilising temperature response (Fig. 9b for ley). Yearly GHG emissions from production of inputs, field operations and soil N balance accumulated in the atmosphere, resulting in increasing RF over time and an increasing warming effect on temperature. For ley, yearly sequestration of additional carbon in soil resulted in increasing RF over time and thus an increasing cooling effect, yet at a declining rate.

4. Discussion

4.1. Crop-specific albedo under regional conditions

This paper presents an approach to identify homogeneous pixels of the MODIS BRDF/Albedo product and to produce climatological albedo for specific crops under regional cultivation conditions. Spatial and temporal variability in crop-specific albedo due to site conditions, management,

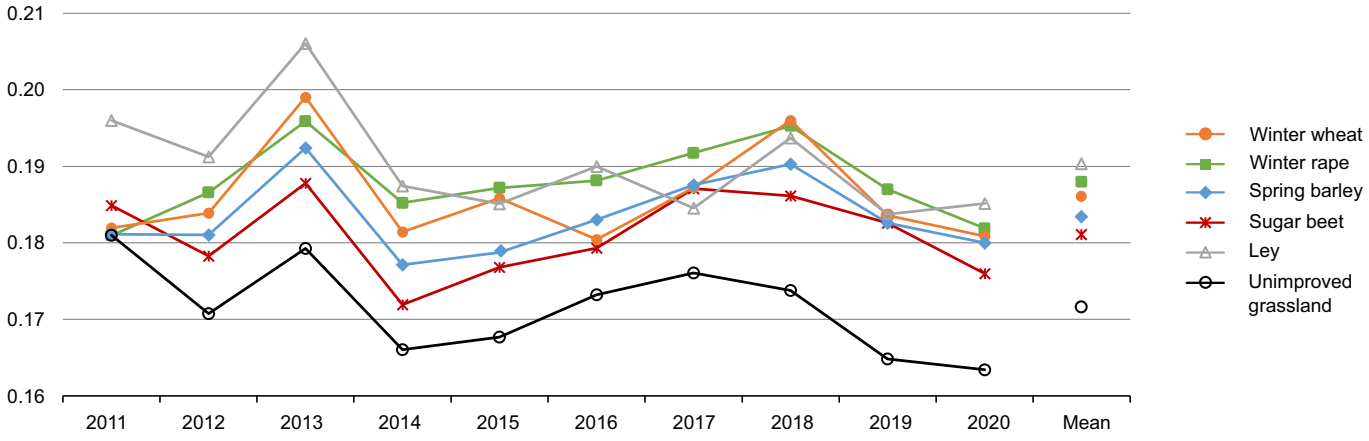

Fig. 7. Annual albedo per agricultural land use in harvest years 2011–2020, and climatological mean across all years.

Table 2
Climate impact of crop cultivation relative to the land reference (unimproved grassland), expressed as GWP_{100} (t CO_2e ha^{-1}). Field operations include production and use of diesel. Inputs include production of fertilisers, pesticides and seeds.

	Inputs	Field operations	Soil N	Soil C	Σ GHG	Albedo	Σ GHG + albedo
Winter wheat	0.78	0.17	1.54	0.18	2.68	−0.23	2.44
Winter rye	0.56	0.17	1.10	0.26	2.08	−0.14	1.94
Winter rape	0.51	0.15	1.18	−0.13	1.71	−0.25	1.46
Spring wheat	0.73	0.16	1.34	0.38	2.61	−0.15	2.46
Spring barley	0.42	0.17	0.80	0.32	1.71	−0.17	1.54
Sugar beet	0.34	0.29	1.27	0.39	2.29	−0.13	2.16
Ley	0.49	0.10	0.96	−0.76	0.79	−0.28	0.51

and yearly weather were captured using satellite observations. Among the 3263 crop-specific pixels identified over a 10-year period, inter-annual variability could be higher than differences between crops in individual years. Nevertheless, differences between crops were largely consistent across years, especially for crops with similar seasonal vegetation cover that experienced comparable albedo effects from temperature and precipitation patterns. Thus comparisons of albedo at crop level should be made taking annual weather into account, particularly anomalies in seasonal snow cover and possibly precipitation. Furthermore, robust observational data are needed to establish representative albedo values that can be used for modelling albedo change and potential climate impacts (e.g. 10 years as in this study, or a typical year). Even small albedo changes can lead to considerable RF at the field scale and quantifiable climate impacts with GWP_{100}. For example, the 0.009 albedo increase under sugar beet resulted in climate cooling of 135 kg CO_2e ha^{-1}.

Similar methods and data to analyse albedo can be used for other agricultural land use types and regions. Yearly GSAA data in Sweden cover 3 million ha of agricultural land, classified into 80 different crop and land use types. Across the EU, farmers declare the use of over 150 million ha. Geodata are increasingly being harmonised and made available under the EU INSPIRE Directive (Directive 2007/2/EC). In Sweden incorrect declarations are rare. The use of crop-specific field polygons avoided ex-post classification of cropland (e.g. Starr et al., 2020), and thus uncertainty was limited to the spatial response of the MODIS product. However, deriving

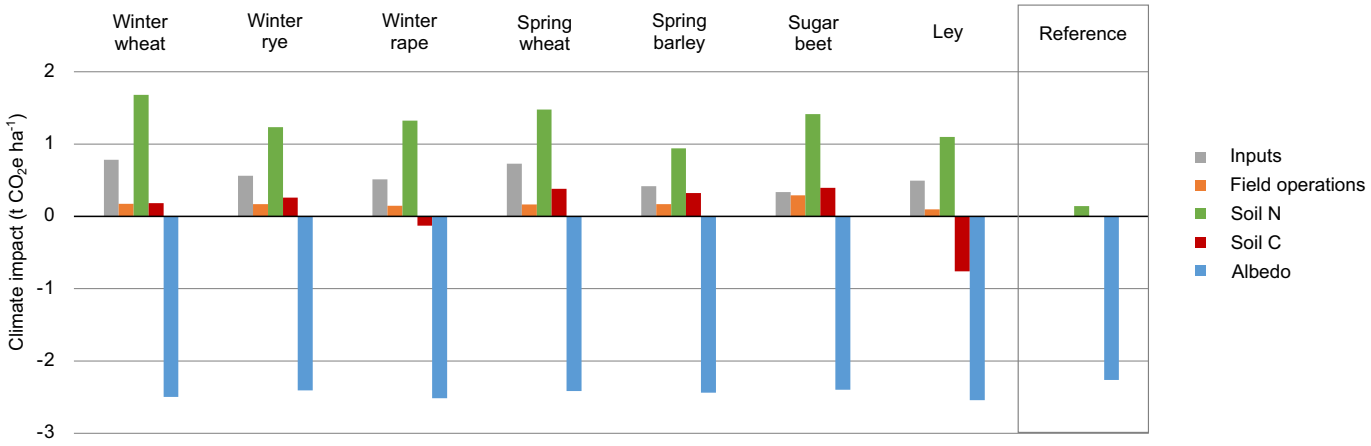

Fig. 8. Absolute climate impact per land use, expressed as GWP_{100} (t CO_2e ha^{-1}). Field operations include production and use of diesel. Inputs include production of fertilisers, pesticides and seeds. Albedo-related cooling is the theoretical potential for increasing albedo relative to a black surface with albedo = 0.

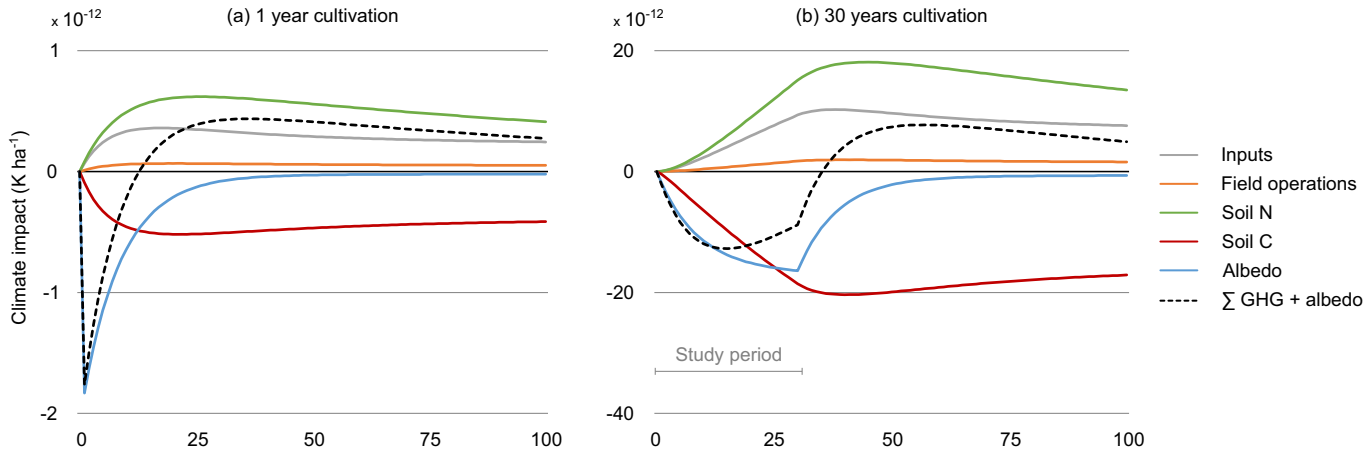

Fig. 9. Time-dependent climate impact (ΔT, K ha^{-1}) of ley production relative to the reference: (a) cultivation during one year and (b) sustained cultivation during 30 years, with no emissions considered after the study period. ΔT is the yearly change in global annual mean surface temperature.

albedo from homogeneous pixels works only for land use types with sufficient spatial coverage. In this study, at least 50 ha were required for 80% pixel purity. Despite sufficient coverage and sample size, results can be biased for land use types that are frequently present close to surfaces with highly contrasting albedo, such as forests or water bodies. The development of observational products with high spatial and temporal resolution will improve the characterisation of surface properties at land use and management level (Duveiller et al., 2011) and increase the possibilities to produce crop-specific albedo using the method presented here, or similar approaches (Starr et al., 2020).

4.2. Importance of albedo change for the climate impact of crop production

A novel approach for systematically including albedo in LCAs of crop production was developed. The methods combine satellite-based albedo, regional data and models to capture regional characteristics of crop production depending on soil type, climate and management practices. The methods were used to calculate and compare climate impacts due to albedo change and GHG fluxes from cultivation of seven major crops in Sweden's southernmost production region. Cultivation of individual crops on current cropland led to albedo increase by 6–11% relative to the reference (climate cooling), and GHG emissions from production of inputs, field operations and soil N_2O formation (climate warming). Soil acted as a carbon sink under ley and rapeseed due to high inputs, and as a CO_2 source under all other crops.

Previous studies showed that land use scenarios can cause similar quantifiable impacts due to albedo and GHGs using GWP_{100} as a metric (e.g. Caiazzo et al., 2014; Carrer et al., 2018; Georgescu et al., 2011; Guardia et al., 2019; Kirschbaum et al., 2013; Sieber et al., 2020). The results in the present study showing that increased albedo countered the GHG impact from production of inputs and field operations by 17–47% of under different crops agree with these findings. However, similar impacts in terms of GWP_{100} (which is based on cumulative RF) can imply substantially different climate outcomes, depending on how RF is distributed over the 100-year period (Fuglestvedt et al., 2003). RF from albedo and GHGs is usually distributed unequally over time in land use scenarios, because albedo affects the Earth's radiative balance as long as it remains changed, whereas GHGs affect it during a long time after emission due to the lasting atmospheric concentration change (Kirschbaum et al., 2013; Sieber et al., 2020). This causes different temperature responses over time. Following a single year of ley cultivation (Fig. 9a), albedo change led to strong temperature effects in the short term, whereas GHG fluxes led to slow onset but more long-lasting effects. The dominating impact of albedo on short timescales was explicit with ΔT, showing that albedo-related cooling countered the GHG-related warming due to production of inputs and field operations by 50%, 8% and 7% in year 20, 50 and 100, respectively. It is important to consider such differences in the timing of impacts from albedo and GHGs in climate change mitigation and adaptation strategies for agricultural land.

The potential to achieve a cooling effect from higher albedo has important implications for crop cultivation. Crops with a long growing season can give increased albedo in spring and autumn on loam soils under wet-temperate climate conditions. The higher potential for albedo-related cooling from perennial ley and winter crops compared with spring-sown crops identified in this study agrees with previous findings showing benefits of growing perennials or cover crops (Lugato et al., 2020; Miller et al., 2016). However, optimal soil coverage in a crop rotation needs to be planned considering agronomic factors such as pre-crop effects, soil and climatic conditions, costs and distribution of workload. In northern Europe, cover crops are less common due to the shorter growing season. Furthermore, the cooling effect from higher albedo is smaller due to low solar irradiance and atmospheric transmittance. To illustrate the importance of seasonal timing, the cooling potential of a year-round albedo increase of 0.01 in PO1 was calculated, and was found to be -128 kg CO_2e ha^{-1} using GWP_{100}. About 80% was obtained between April and August, and the impact per day was almost 30 times higher in June than in December (Fig. 10). Consequently, a cover crop growing from September to March

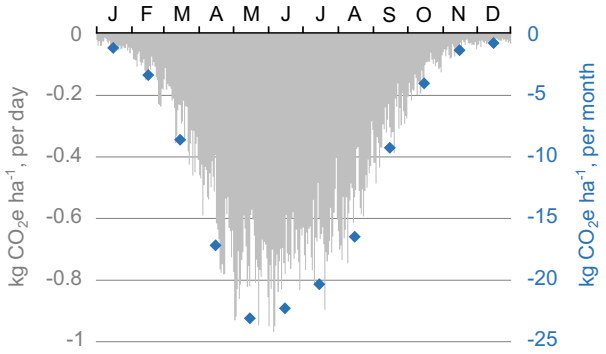

Fig. 10. Climate impact of a 0.01 albedo increase using GWP_{100} (kg CO_2e ha^{-1}) with albedo change sustained for one day (left axis) or one month (right axis).

increases albedo during the least effective period. Potential cooling from increased albedo needs to be balanced against GHG emissions, other environmental impacts, and direct and indirect consequences for crop production and use.

4.3. Uncertainties of land use effects

In the LCA, climate impacts due to albedo change, soil C and soil N balance were included, considering regional conditions. Effects of land use are often omitted in LCAs, or quantified using generic literature data and emission factors such as IPCC Tier 1 methods (Goglio et al., 2015; Henryson et al., 2020; Muñoz et al., 2010). These methods are attractive because they are transparent and simple to use, with high availability of input data and comparability of LCA results across studies. However, they fail to reflect the complexity of land use effects at field level due to dependence on soil properties, climate, crop characteristics and management, and intra-annual interactions between them. LCA studies would benefit from better estimates of land use effects. Some studies used dynamic (process-based) crop-climate-soil models to generate inventory data and thereby reduced the uncertainty of emissions from specific fields (e.g. Bessou et al., 2013; Goglio et al., 2014). The realistic representation of albedo in such models is a nontrivial task in itself (see e.g. Bagley et al., 2015). However, site-specific results may not be representative of typical crop production in a region, which is of interest in many LCA applications, and dynamic modelling at larger scale requires extensive amounts of input data. Since the purpose of many LCAs is to assess potential differences in climate impact among agricultural practices or systems, inventory modelling should reflect the probable average effects rather than reproducing actual effects in a single field and year (Cederberg et al., 2013). As a compromise, most agricultural LCA research uses site-dependent approaches that partly account for local or regional conditions, in agreement with the study objectives (Goglio et al., 2015).

In the present study, N_2O emissions estimated with IPCC Tier 1–2 methods involved considerable uncertainty. This uncertainty includes plausible variability in field-level emissions and insufficient spatial differentiation. However, site-dependent models that account for soil properties, climate and crop do not necessarily produce more useful results (Henryson et al., 2020). Modelled soil carbon changes were consistent with the projected trend in PO1 under current agricultural practices (Andrén et al., 2008), when considering the fractional area of major crops and the omitted C input from manure application. The use of observational albedo data introduced unwanted variation due to management practices that were not included in the scenarios, but are employed by farmers in the region. For instance, ley cultivation in PO1 is performed not only with mineral fertilisation and mowing as in our scenario, but also with manure application and partial grazing. Because the fractional representation of management practices in the albedo data could not be quantified, the crop-specific albedo values represented an anonymous mix of practices

performed at large scale. This resulted in a common inconsistency in inventory data, by using scenario-specific data if available and generic data otherwise.

Besides the uncertainties associated with albedo, soil C and N balance under individual land uses, there is no consensus on how the divergence from the potential natural state of the land should be considered and attributed to crop cultivation in LCA. This conceptual difficulty is related to defining a suitable land reference, the temporal scope for the study and the timeframe for assessing climate impacts (Koponen et al., 2018). The time-dependent approach in this study was limited to fluxes that actually occur during crop cultivation, due to yearly changes in carbon stocks on current cropland and albedo change relative to unused land. The definition of the land reference is debatable, e.g. deciduous forest could have been chosen, likely resulting in lower reference albedo and thus higher albedo increase under crops. Other methods account for impacts of land transformation and/or delayed regeneration and attribute hypothetical fluxes to land use, e.g. IPCC Tier 1–2, and methods proposed by Müller-Wenk and Brandão (2010), Schmidinger and Stehfest (2012), Muñoz et al. (2010) and Bright et al. (2012). These methods operate with amortisation periods to allocate the effects of one-time interventions over time and/or simplified assumptions about regeneration over time.

The present study included albedo, but land use also alters other biophysical land cover properties, such as evapotranspiration efficiency and surface roughness, that influence the climate predominantly at local and regional scale (IPCC, 2019b). Locally, biophysical effects of land use for crop production can meet or exceed the temperature change induced by globally rising GHG concentrations (Georgescu et al., 2011). However, interdependencies of various surface fluxes and environmental conditions complicate the relationship between crops and local climate impacts (Bagley et al., 2014), and the attribution of changes in temperature, precipitation and other climate variables to specific land use activities (Bright et al., 2015). There is also no consensus on how to compare local biophysical effects and global-scale GHG impacts with a common metric.

When moving from GHG-centric accounting to more comprehensive assessments of land use climate impacts, albedo is increasingly considered because its first-order radiative effects can be directly included in impact assessments using RF-based metrics. A drawback is that albedo change generally does not lead to the same global temperature effect per unit RF as CO_2 (Bright et al., 2015), depending on its spatial distribution and rapid adjustments occurring in the troposphere such as changes in temperature, water vapour and clouds (Hansen et al., 2005; Richardson et al., 2019). Effective radiative forcing, i.e. RF after tropospheric adjustments, is suggested to be a better predictor of global mean temperature, but its computation requires complex modelling. Further research and metric development is needed to adequately account for the disparate climate response to RF from albedo change and CO_2 (Bright and Lund, 2021).

4.4. Perspectives

The methods developed for studying life cycle climate impacts due to albedo and GHGs can be applied to other agricultural production regions and land use scenarios. Evaluating climate impacts by system component and over time makes it easier to explain the effects of agricultural land use and, more importantly, when these effects occur. The scenario results obtained for one year of cultivation can be recombined to evaluate individual land uses (e.g. winter wheat vs. spring wheat), cultivation of crops in a rotation, or sustained cultivation in a landscape.

The methods and data presented in this paper could contribute to a framework for systematically evaluating the climate impact of different agricultural land uses and management options. Such systematic evaluations can help inform future strategies on how to provide sufficient biomass for food, feed, energy and biomaterials, while simultaneously contributing to climate goals. The methods complement existing approaches such as a recently developed tool for assessing local biophysical effects of land cover change with a tiered approach (Duveiller et al., 2020). The present study addressed land use decisions that do not lead to land cover transition, included consequences across the life cycle and quantified global climate impacts based on RF. Future research could integrate different approaches and provide practical guidance at the level of agricultural land use and management practices, considering both locally-induced and RF-based effects. Trade-offs should be avoided by including different forcing agents, short-term and long-term impacts, local and global impacts, and direct and indirect consequences of from a systems perspective.

CRediT authorship contribution statement

Petra Sieber: Conceptualization, Methodology, Software, Investigation, Formal analysis, Validation, Visualization, Writing – original draft, Writing – review & editing. **Niclas Ericsson:** Conceptualization, Supervision, Validation, Writing – review & editing. **Torun Hammar:** Conceptualization, Supervision, Validation, Writing – review & editing. **Per-Anders Hansson:** Funding acquisition, Conceptualization, Supervision, Validation, Writing – review & editing.

Declaration of competing interest

The authors declare that they have no known competing financial interests or personal relationships that could have appeared to influence the work reported in this paper.

Acknowledgements

This work was supported by the Swedish Strategic Research Programme STandUP for Energy. The authors thank Martin Bolinder and Thomas Kätterer (Dept. of Ecology, SLU) for contributing expertise on soil carbon modelling. The results contain modified Copernicus Climate Change Service information 2020.

Appendix A. Supplementary data

Supplementary data to this article can be found online at https://doi.org/10.1016/j.scitotenv.2022.155455.

References

Andrén, O., Kätterer, T., Karlsson, T., 2004. ICBM regional model for estimations of dynamics of agricultural soil carbon pools. Nutr. Cycl. Agroecosyst. 70 (2), 231–239. https://doi.org/10.1023/B:FRES.0000048471.59164.ff.

Andrén, O., Kätterer, T., Karlsson, T., Eriksson, J., 2008. Soil C balances in Swedish agricultural soils 1990–2004, with preliminary projections. Nutr. Cycl. Agroecosyst. 81 (2), 129–144. https://doi.org/10.1007/s10705-008-9177-z.

Bagley, J.E., Davis, S.C., Georgescu, M., Hussain, M.Z., Miller, J., Nesbitt, S.W., VanLoocke, A., Bernacchi, C.J., 2014. The biophysical link between climate, water, and vegetation in bioenergy agro-ecosystems. Biomass Bioenergy 71, 187–201. https://doi.org/10.1016/j.biombioe.2014.10.007.

Bagley, J.E., Miller, J., Bernacchi, C.J., 2015. Biophysical impacts of climate-smart agriculture in the Midwest United States. Plant Cell Environ. 38 (9), 1913–1930. https://doi.org/10.1111/pce.12485.

Bessou, C., Lehuger, S., Gabrielle, B., Mary, B., 2013. Using a crop model to account for the effects of local factors on the LCA of sugar beet ethanol in Picardy region, France. Int. J. Life Cycle Assess. 18 (1), 24–36. https://doi.org/10.1007/s11367-012-0457-0.

Betts, R.A., 2000. Offset of the potential carbon sink from boreal forestation by decreases in surface albedo. Nature 408 (6809), 187–190. https://doi.org/10.1038/35041545.

Betts, R.A., Falloon, P.D., Goldewijk, K.K., Ramankutty, N., 2007. Biogeophysical effects of land use on climate: model simulations of radiative forcing and large-scale temperature change. Agric. For. Meteorol. 142 (2–4), 216–233. https://doi.org/10.1016/j.agrformet.2006.08.021.

Bright, R.M., Lund, M.T., 2021. CO2-equivalence metrics for surface albedo change based on the radiative forcing concept: a critical review. Atmos. Chem. Phys. 21 (12), 9887–9907. https://doi.org/10.5194/acp-21-9887-2021.

Brandão, M., Milà i Canals, L., Clift, R., 2011. Soil organic carbon changes in the cultivation of energy crops: implications for GHG balances and soil quality for use in LCA. Biomass Bioenergy 35 (6), 2323–2336. https://doi.org/10.1016/j.biombioe.2009.10.019.

Bright, R.M., Cherubini, F., Stromman, A.H., 2012. Climate impacts of bioenergy: inclusion of carbon cycle and albedo dynamics in life cycle impact assessment. Environ. Impact Assess. Rev. 37, 2–11. https://doi.org/10.1016/j.eiar.2012.01.002.

Bright, R.M., Zhao, K.G., Jackson, R.B., Cherubini, F., 2015. Quantifying surface albedo and other direct biogeophysical climate forcings of forestry activities. Glob. Chang. Biol. 21 (9), 3246–3266. https://doi.org/10.1111/gcb.12951.

Caiazzo, F., Malina, R., Staples, M.D., Wolfe, P.J., Yim, S.H.L., Barrett, S.R.H., 2014. Quantifying the climate impacts of albedo changes due to biofuel production: a comparison with biogeochemical effects. Environ. Res. Lett. 9 (2). https://doi.org/10.1088/1748-9326/9/2/024015.

Campagnolo, M.L., Montaño, E.L., 2014. Estimation of effective resolution for daily MODIS gridded surface reflectance products. IEEE Trans. Geosci. Remote Sens. 52 (9), 5622–5632. https://doi.org/10.1109/TGRS.2013.2291496.

Campagnolo, M.L., Sun, Q., Liu, Y., Schaaf, C., Wang, Z., Román, M.O., 2016. Estimating the effective spatial resolution of the operational BRDF, albedo, and nadir reflectance products from MODIS and VIIRS. Remote Sens. Environ. 175, 52–64. https://doi.org/10.1016/j.rse.2015.12.033.

Carrer, D., Pique, G., Ferlicoq, M., Ceamanos, X., Ceschia, E., 2018. What is the potential of cropland albedo management in the fight against global warming? A case study based on the use of cover crops. Environ. Res. Lett. 13 (4). https://doi.org/10.1088/1748-9326/aab650.

Cederberg, C., Henriksson, M., Berglund, M., 2013. An LCA researcher's wish list – data and emission models needed to improve LCA studies of animal production. Animal 7, 212–219. https://doi.org/10.1017/S1751731113000785.

Chang, J., Ciais, P., Gasser, T., Smith, P., Herrero, M., Havlík, P., Obersteiner, M., Guenet, B., Goll, D.S., Li, W., Naipal, V., Peng, S., Qiu, C., Tian, H., Viovy, N., Yue, C., Zhu, D., 2021. Climate warming from managed grasslands cancels the cooling effect of carbon sinks in sparsely grazed and natural grasslands. Nat. Commun. 12 (1), 118. https://doi.org/10.1038/s41467-020-20406-7.

Davin, E.L., de Noblet-Ducoudré, N., 2010. Climatic impact of global-scale deforestation: Radiative versus Nonradiative processes. J. Clim. 23 (1), 97–112. https://doi.org/10.1175/2009JCLI3102.1.

Davin, E.L., Seneviratne, S.I., Ciais, P., Olioso, A., Wang, T., 2014. Preferential cooling of hot extremes from cropland albedo management. Proc. Natl. Acad. Sci. U. S. A. 111 (27), 9757–9761. https://doi.org/10.1073/pnas.1317323111.

Donohoe, A., Battisti, D.S., 2011. Atmospheric and surface contributions to planetary albedo. J. Clim. 24 (16), 4402–4418. https://doi.org/10.1175/2011jcli3946.1.

Donohoe, A., Blanchard-Wrigglesworth, E., Schweiger, A., Rasch, P.J., 2020. The effect of atmospheric Transmissivity on model and observational estimates of the sea ice albedo feedback. J. Clim. 33 (13), 5743–5765. https://doi.org/10.1175/jcli-d-19-0674.1.

Duveiller, G., Baret, F., Defourny, P., 2011. Crop specific green area index retrieval from MODIS data at regional scale by controlling pixel-target adequacy. Remote Sens. Environ. 115 (10), 2686–2701. https://doi.org/10.1016/j.rse.2011.05.026.

Duveiller, G., Hooker, J., Cescatti, A., 2018. The mark of vegetation change on Earth's surface energy balance. Nat. Commun. 9 (1), 679. https://doi.org/10.1038/s41467-017-02810-8.

Duveiller, G., Caporaso, L., Abad-Viñas, R., Perugini, L., Grassi, G., Arneth, A., Cescatti, A., 2020. Local biophysical effects of land use and land cover change: towards an assessment tool for policy makers. Land Use Policy 91, 104382. https://doi.org/10.1016/j.landusepol.2019.104382.

Erb, K.-H., Luyssaert, S., Meyfroidt, P., Pongratz, J., Don, A., Kloster, S., Kuemmerle, T., Fetzel, T., Fuchs, R., Herold, M., Haberl, H., Jones, C.D., Marín-Spiotta, E., McCallum, I., Robertson, E., Seufert, V., Fritz, S., Valade, A., Wiltshire, A., Dolman, A.J., 2017. Land management: data availability and process understanding for global change studies. Glob. Chang. Biol. 23 (2), 512–533. https://doi.org/10.1111/gcb.13443.

Ericsson, N., Porsö, C., Ahlgren, S., Nordberg, A., Sundberg, C., Hansson, P.-A., 2013. Time-dependent climate impact of a bioenergy system - methodology development and application to Swedish conditions. GCB Bioenergy 5 (5), 580–590. https://doi.org/10.1111/gcbb.12031.

Friedl, M., Sulla-Menashe, D., 2019. *MCD12Q1 MODIS/Terra + aqua land cover type yearly L3 global 500m SIN grid V006* [online dataset]. NASA EOSDIS Land Processes DAAC https://doi.org/10.5067/MODIS/MCD12Q1.006.

Fuglestvedt, J.S., Berntsen, T.K., Godal, O., Sausen, R., Shine, K.P., Skodvin, T., 2003. Metrics of climate change: assessing radiative forcing and emission indices. Clim. Chang. 58 (3), 267–331. https://doi.org/10.1023/A:1023905326842.

Gao, F., Schaaf, C.B., Strahler, A.H., Roesch, A., Lucht, W., Dickinson, R., 2005. MODIS bidirectional reflectance distribution function and albedo climate modeling grid products and the variability of albedo for major global vegetation types. J. Geophys. Res. Atmos. 110 (D1). https://doi.org/10.1029/2004JD005190.

Georgescu, M., Lobell, D.B., Field, C.B., 2011. Direct climate effects of perennial bioenergy crops in the United States. Proc. Natl. Acad. Sci. U. S. A. 108 (11), 4307–4312. https://doi.org/10.1073/pnas.1008779108.

Goglio, P., Grant, B.B., Smith, W.N., Desjardins, R.L., Worth, D.E., Zentner, R., Malhi, S.S., 2014. Impact of management strategies on the global warming potential at the cropping system level. Sci. Total Environ. 490, 921–933. https://doi.org/10.1016/j.scitotenv.2014.05.070.

Goglio, P., Smith, W.N., Grant, B.B., Desjardins, R.L., McConkey, B.G., Campbell, C.A., Nemecek, T., 2015. Accounting for soil carbon changes in agricultural life cycle assessment (LCA): a review. J. Clean. Prod. 104, 23–39. https://doi.org/10.1016/j.jclepro.2015.05.040.

Guardia, G., Aguilera, E., Vallejo, A., Sanz-Cobena, A., Alonso-Ayuso, M., Quemada, M., 2019. Effective climate change mitigation through cover cropping and integrated fertilization: a global warming potential assessment from a 10-year field experiment. J. Clean. Prod. 241, 118307. https://doi.org/10.1016/j.jclepro.2019.118307.

Hansen, J., Sato, M., Ruedy, R., Nazarenko, L., Lacis, A., Schmidt, G.A., Russell, G., Aleinov, I., Bauer, M., Bauer, S., Bell, N., Cairns, B., Canuto, V., Chandler, M., Cheng, Y., Del Genio, A., Faluvegi, G., Fleming, E., Friend, A., Hall, T., Jackman, C., Kelley, M., Kiang, N., Koch, D., Lean, J., Lerner, J., Lo, K., Menon, S., Miller, R., Minnis, P., Novakov, T., Oinas, V., Perlwitz, J., Perlwitz, J., Rind, D., Romanou, A., Shindell, D., Stone, P., Sun, S., Tausnev, N., Thresher, D., Wielicki, B., Wong, T., Yao, M., Zhang, S., 2005. Efficacy of climate forcings. J. Geophys. Res.-Atmos. 110 (D18). https://doi.org/10.1029/2005jd005776.

Henryson, K., Kätterer, T., Tidåker, P., Sundberg, C., 2020. Soil N2O emissions, N leaching and marine eutrophication in life cycle assessment – a comparison of modelling approaches. Sci. Total Environ. 725, 138332. https://doi.org/10.1016/j.scitotenv.2020.138332.

Hersbach, H., Bell, B., Berrisford, P., Horányi, A., Muñoz Sabater, J., Nicolas, J., Radu, R., Schepers, D., Simmons, A., Soci, C., Dee, D., 2018. *ERA5* hourly data on single levels from 1979 to present [online dataset]. Copernicus Climate Change Service (C3S) Climate Data Store (CDS) https://doi.org/10.24381/cds.adbb2d47.

Hovi, A., Lindberg, E., Lang, M., Arumäe, T., Peuhkurinen, J., Sirparanta, S., Pyankov, S., Rautiainen, M., 2019. Seasonal dynamics of albedo across European boreal forests: analysis of MODIS albedo and structural metrics from airborne LiDAR. Remote Sens. Environ. 224, 365–381. https://doi.org/10.1016/j.rse.2019.02.001.

IPCC, 2019. 2019 Refinement to the 2006 IPCC Guidelines for National Greenhouse gas Inventories. IGES, Hayama, Japan.

IPCC, 2019b. In: Shukla, P.R., Skea, J., Buendia, E. Calvo, Masson-Delmotte, V., Pörtner, H.-O., Roberts, D.C., Zhai, P., Slade, R., Connors, S., van Diemen, R., Ferrat, M., Haughey, E., Luz, S., Neogi, S., Pathak, M., Petzold, J., Pereira, J. Portugal, Vyas, P., Huntley, E., Kissick, K., Belkacemi, M., Malley, J. (Eds.), Climate Change and Land: an IPCC Special Report on Climate Change, Desertification, Land Degradation, Sustainable Land Management, Food Security, and Greenhouse Gas Fluxes in Terrestrial Ecosystems.

Jordahl, K., Bossche, J. V.d, Fleischmann, M., Wasserman, J., McBride, J., Gerard, J., Tratner, J., Perry, M., Badaracco, A.G., Farmer, C., Hjelle, G.A., Snow, A.D., Cochran, M., Gillies, S., Culbertson, L., Bartos, M., Eubank, N. maxalbert, Bilogur, A., Rey, S., Ren, C., Arribas-Bel, D., Wasser, L., Wolf, L.J., Journois, M., Wilson, J., Greenhall, A., Holdgraf, C., Filipe, Leblanc, F., 2020. Geopandas/Geopandas: v0.8.1 (Version v0.8.1). Zenodo https://doi.org/10.5281/zenodo.3946761.

Kätterer, T., Andersson, L., Andrén, O., Persson, J., 2008. Long-term impact of chronosequential land use change on soil carbon stocks on a Swedish farm. Nutr. Cycl. Agroecosyst. 81 (2), 145. https://doi.org/10.1007/s10705-007-9156-9.

Kaye, J.P., Quemada, M., 2017. Using cover crops to mitigate and adapt to climate change. A review. Agron. Sustain. Dev. 37 (1), 4. https://doi.org/10.1007/s13593-016-0410-x.

Kim, D.-G., Giltrap, D., Hernandez-Ramirez, G., 2013. Erratum to: background nitrous oxide emissions in agricultural and natural lands: a meta-analysis. Plant Soil 373 (1), 1007–1008. https://doi.org/10.1007/s11104-013-1883-x.

Kirschbaum, M.U.F., Saggar, S., Tate, K.R., Thakur, K.P., Giltrap, D.L., 2013. Quantifying the climate-change consequences of shifting land use between forest and agriculture. Sci. Total Environ. 465, 314–324. https://doi.org/10.1016/j.scitotenv.2013.01.026.

Koponen, K., Soimakallio, S., Kline, K.L., Cowie, A., Brandão, M., 2018. Quantifying the climate effects of bioenergy – choice of reference system. Renew. Sust. Energ. Rev. 81, 2271–2280. https://doi.org/10.1016/j.rser.2017.05.292.

Kvarmo, P., Emelie, A., Börling, K., Hjelm, E., Jonsson, P., Listh, U., Malgeryd, J., 2019. Rekommendationer för gödsling och kalkning 2020 (Recommendations for fertilisation and calcination 2020). Swedish Board of Agriculture, Jönköping, Sweden.

Lewis, P., Barnsley, M., 1994. Influence of the Sky Radiance Distribution on Various Formulations of the Earth Surface Albedo Paper presented at the Proc. Conf. Phys. Meas. Sign. Remote Sens., Val d'Isere, France.

Liu, J., Schaaf, C., Strahler, A., Jiao, Z., Shuai, Y., Zhang, Q., Roman, M., Augustine, J.A., Dutton, E.G., 2009. Validation of moderate resolution imaging Spectroradiometer (MODIS) albedo retrieval algorithm: dependence of albedo on solar zenith angle. J. Geophys. Res. Atmos. 114 (D1). https://doi.org/10.1029/2008jd009969.

Lucht, W., Schaaf, C., Strahler, A.H., 2000. An algorithm for the retrieval of albedo from space using semiempirical BRDF models. IEEE Trans. Geosci. Remote Sens. 38 (2), 977–998. https://doi.org/10.1109/36.841980.

Lugato, E., Cescatti, A., Jones, A., Ceccherini, G., Duveiller, G., 2020. Maximising climate mitigation potential by carbon and radiative agricultural land management with cover crops. Environ. Res. Lett. 15 (9), 094075. https://doi.org/10.1088/1748-9326/aba137.

Mahmood, R., Pielke, R.A., Hubbard, K.G., Niyogi, D., Dirmeyer, P.A., McAlpine, C., Carleton, A.M., Hale, R., Gameda, S., Beltran-Przekurat, A., Baker, B., McNider, R., Legates, D.R., Shepherd, M., Du, J.Y., Blanken, P.D., Frauenfeld, O.W., Nair, U.S., Fall, S., 2014. Land cover changes and their biogeophysical effects on climate. Int. J. Climatol. 34 (4), 929–953. https://doi.org/10.1002/joc.3736.

Marland, G., Pielke, R.A., Apps, M., Avissar, R., Betts, R.A., Davis, K.J., Frumhoff, P.C., Jackson, S.T., Joyce, L.A., Kauppi, P., Katzenberger, J., MacDicken, K.G., Neilson, R.P., Niles, J.O., Niyogi, D.d.S., Norby, R.J., Pena, N., Sampson, N., Xue, Y., 2003. The climatic impacts of land surface change and carbon management, and the implications for climate-change mitigation policy. Clim. Pol. 3 (2), 149–157. https://doi.org/10.3763/cpol.2003.0318.

Miller, J.N., VanLoocke, A., Gomez-Casanovas, N., Bernacchi, C.J., 2016. Candidate perennial bioenergy grasses have a higher albedo than annual row crops. GCB Bioenergy 8 (4), 818–825. https://doi.org/10.1111/gcbb.12291.

Müller-Wenk, R., Brandão, M., 2010. Climatic impact of land use in LCA—carbon transfers between vegetation/soil and air. Int. J. Life Cycle Assess. 15 (2), 172–182. https://doi.org/10.1007/s11367-009-0144-y.

Muñoz, I., Campra, P., Fernández-Alba, A.R., 2010. Including CO2-emission equivalence of changes in land surface albedo in life cycle assessment. Methodology and case study on greenhouse agriculture. *The*. Int. J. Life Cycle Assess. 15 (7), 672–681. https://doi.org/10.1007/s11367-010-0202-5.

Myhre, G., Kvalevåg, M.M., Schaaf, C.B., 2005. Radiative forcing due to anthropogenic vegetation change based on MODIS surface albedo data. Geophys. Res. Lett. 32 (21). https://doi.org/10.1029/2005GL024004.

Myhre, G., Shindell, D., Breón, F.-M., Collins, W., Fuglestvedt, J., Huang, J., Koch, D., Lamarque, J., Lee, D., Mendoza, B., Nakajima, T., Robock, A., Stephens, G., Takemura, T., Zhang, H., 2013. Anthropogenic and natural Radiative forcing. In: Stocker, T.F., Qin, D., Plattner, G.-K., Tignor, M., Allen, S.K., Boschung, J., Nauels, A., Xia, Y., Bex, V., Midgley, P.M. (Eds.), Climate Change 2013: The Physical Science Basis. Contribution

of Working Group I to the Fifth Assessment Report of the Intergovernmental Panel on Climate Change. Cambridge University Press, Cambridge and New York, NY, pp. 659–740.
Pielke, R.A., Avissar, R., Raupach, M., Dolman, A.J., Zeng, X.B., Denning, A.S., 1998. Interactions between the atmosphere and terrestrial ecosystems: influence on weather and climate. Glob. Chang. Biol. 4 (5), 461–475. https://doi.org/10.1046/j.1365-2486.1998.t01-1-00176.x.
Pielke, R.A., Marland, G., Betts, R.A., Chase, T.N., Eastman, J.L., Niles, J.O., Niyogi, D.D.S., Running, S.W., 2002. The influence of land-use change and landscape dynamics on the climate system: relevance to climate-change policy beyond the radiative effect of greenhouse gases. Philosophical Transactions of the Royal Society of London Series a. Mathematical Physical and Engineering Sciences 360 (1797), 1705–1719. https://doi.org/10.1098/rsta.2002.1027.
Qu, Y., Liang, S., Liu, Q., He, T., Liu, S., Li, X., 2015. Mapping surface broadband albedo from satellite observations: a review of literatures on algorithms and products. Remote Sens. 7 (1), 990–1020. https://doi.org/10.3390/rs70100990.
Richardson, T.B., Forster, P.M., Smith, C.J., Maycock, A.C., Wood, T., Andrews, T., Boucher, O., Faluvegi, G., Fläschner, D., Hodnebrog, Ø., Kasoar, M., Kirkevåg, A., Lamarque, J.-F., Mülmenstädt, J., Myhre, G., Olivié, D., Portmann, R.W., Samset, B.H., Shawki, D., Shindell, D., Stier, P., Takemura, T., Voulgarakis, A., Watson-Parris, D., 2019. Efficacy of climate Forcings in PDRMIP models. J. Geophys. Res. Atmos. 124 (23), 12824–12844. https://doi.org/10.1029/2019JD030581.
Sagris, V., Wojda, P., Milenov, P., Devos, W., 2013. The harmonised data model for assessing land parcel identification systems compliance with requirements of direct aid and Agri-environmental schemes of the CAP. J. Environ. Manag. 118, 40–48. https://doi.org/10.1016/j.jenvman.2012.12.019.
Schaaf, C.B., Wang, Z., 2015. *MCD43A1 MODIS/Terra+aqua BRDF/albedo model parameters daily L3 global - 500m V006* [online dataset]. NASA EOSDIS Land Processes DAAC. https://doi.org/10.5067/MODIS/MCD43A1.006.
Schaaf, C.B., Gao, F., Strahler, A.H., Lucht, W., Li, X., Tsang, T., Strugnell, N.C., Zhang, X., Jin, Y., Muller, J.-P., Lewis, P., Barnsley, M., Hobson, P., Disney, M., Roberts, G., Dunderdale, M., Doll, C., d'Entremont, R.P., Hu, B., Liang, S., Privette, J.L., Roy, D., 2002. First operational BRDF, albedo nadir reflectance products from MODIS. Remote Sens. Environ. 83 (1), 135–148. https://doi.org/10.1016/S0034-4257(02)00091-3.
Schmidinger, K., Stehfest, E., 2012. Including CO2 implications of land occupation in LCAs—method and example for livestock products. Int. J. Life Cycle Assess. 17 (8), 962–972. https://doi.org/10.1007/s11367-012-0434-7.
Sieber, P., Ericsson, N., Hammar, T., Hansson, P.-A., 2020. Including albedo in time-dependent LCA of bioenergy. GCB Bioenergy 12 (6), 410–425. https://doi.org/10.1111/gcbb.12682.
Singarayer, J.S., Davies-Barnard, T., 2012. Regional climate change mitigation with crops: context and assessment. Philos. Trans. R. Soc. A Math. Phys. Eng. Sci. 370 (1974), 4301–4316. https://doi.org/10.1098/rsta.2012.0010.
Smith, P., Davis, S.J., Creutzig, F., Fuss, S., Minx, J., Gabrielle, B., Kato, E., Jackson, R.B., Cowie, A., Kriegler, E., van Vuuren, D.P., Rogelj, J., Ciais, P., Milne, J., Canadell, J.G., McCollum, D., Peters, G., Andrew, R., Krey, V., Shrestha, G., Friedlingstein, P., Gasser, T., Grübler, A., Heidug, W.K., Jonas, M., Jones, C.D., Kraxner, F., Littleton, E., Lowe, J., Moreira, J.R., Nakicenovic, N., Obersteiner, M., Patwardhan, A., Rogner, M., Rubin, E., Sharifi, A., Torvanger, A., Yamagata, Y., Edmonds, J., Yongsung, C., 2016. Biophysical and economic limits to negative CO2 emissions. Nat. Clim. Chang. 6 (1), 42–50. https://doi.org/10.1038/nclimate2870.
Starr, J., Zhang, J., Reid, J.S., Roberts, D.C., 2020. Albedo impacts of changing agricultural practices in the United States through space-borne analysis. Remote Sens. 12 (18), 2887. https://doi.org/10.3390/rs12182887.
Statistics Sweden, 2020a. Standard yields for yield survey districts, counties and the whole country in 2020 (JO 15 SM 2001). Retrieved from https://www.scb.se/publikation/40603.
Statistics Sweden, 2020b. Use of agricultural land 2011–2020. Retrieved 2021-01-17 http://www.scb.se/jo0104-en.
Stephens, G.L., O'Brien, D., Webster, P.J., Pilewski, P., Kato, S., Li, J.L., 2015. The albedo of earth. Rev. Geophys. 53 (1), 141–163. https://doi.org/10.1002/2014rg000449.
Sütterlin, M., Stöckli, R., Schaaf, C.B., Wunderle, S., 2016. Albedo climatology for European land surfaces retrieved from AVHRR data (1990–2014) and its spatial and temporal analysis from green-up to vegetation senescence. J. Geophys. Res. Atmos. 121 (14), 8156–8171. https://doi.org/10.1002/2016JD024933.
Swedish Board of Agriculture, 2020. *Geospatial aid application data, 2011-2020* [Vector dataset].
Swedish EPA, 2019. National Inventory Report Sweden 2020. Greenhouse Gas Emission Inventories 1990–2018. Submitted under the United Nations Framework Convention on Climate Change and the Kyoto Protocol Retrieved from https://unfccc.int/documents/224123.
Velthof, G.L., Lesschen, J.P., Schils, R.L.M., Smit, A., Elbersen, B.S., Hazeu, G.W., Mucher, C.A., Oenema, O., 2014. Grassland areas, production and use. Retrieved from https://ec.europa.eu/eurostat/documents/2393397/8259002/Grassland_2014_Final+report.pdf/58aca1dd-de6f-4880-a48e-1331cafae297.
Wang, D., Liang, S., He, T., Yu, Y., Schaaf, C., Wang, Z., 2015. Estimating daily mean land surface albedo from MODIS data. J. Geophys. Res.-Atmos. 120 (10), 4825–4841. https://doi.org/10.1002/2015jd023178.
Wang, Z., Schaaf, C.B., Sun, Q., Shuai, Y., Román, M.O., 2018. Capturing rapid land surface dynamics with collection V006 MODIS BRDF/NBAR/albedo (MCD43) products. Remote Sens. Environ. 207, 50–64. https://doi.org/10.1016/j.rse.2018.02.001.
Wickham, J., Barnes, C.A., Nash, M.S., Wade, T.G., 2015. Combining NLCD and MODIS to create a land cover-albedo database for the continental United States. Remote Sens. Environ. https://doi.org/10.1016/j.rse.2015.09.012.
Winton, M., 2005. Simple optical models for diagnosing surface-atmosphere shortwave interactions. J. Clim. 18 (18), 3796–3805. https://doi.org/10.1175/jcli3502.1.
Zhao, K., Jackson, R.B., 2014. Biophysical forcings of land-use changes from potential forestry activities in North America. Ecol. Monogr. 84 (2), 329–353. https://doi.org/10.1890/12-1705.1.